Technobius, 2026, 6(4), 0111, DOI: https://doi.org/10.54355/tbus/27897338.6.4.0111

Technobius

https://technobius.kz/

e-ISSN 2789-7338

Article

Cement-reduced ternary concrete with fly ash and silica fume for irrigation canal structures: computational mix design with single-composition experimental verification

Zhuldyz Baikhojayeva[1,*], Daniyar Akhmetov[1], Khrystyna Moskalova[2]

[1]Department of Construction and Building Materials, Satbayev University, Almaty, Kazakhstan
[2]Development and Training Centre for the Metal Industry – Metal Centre Čakovec, Čakovec, Croatia
*Correspondence: baikhojayeva.z@stud.satbayev.university

Abstract. Irrigation canal linings in Kazakhstan face freeze-thaw cycling, sulfate-bearing water, and abrasive sediment flow, while national programs to rehabilitate more than 14,000 km of canals create sustained demand for lower-clinker concrete. This study computationally designs a cement-reduced ternary binder (CEM I 42.5N, Ekibastuz low-calcium fly ash, and DSF-95 silica fume, 70:20:10 by mass) that replaces 30% of the cement in a plant control mixture (280 vs 400 kg/m3) while preserving total binder content, paste volume, and aggregate skeleton. The design combines particle-packing simulation, a modified Bolomey model calibrated on the measured plant control (R_{28} = 44.5 MPa), and Powers-model porosity. Experimentally, a laboratory composition with the same ternary binder proportions was cast and tested in 100 mm cubes, yielding a measured R28 of 52.8 MPa versus 52.6 MPa predicted (0.4% deviation); its fracture surface was examined by scanning electron microscopy. The predicted ternary mixture reaches R_{28} = 55.2 MPa (+24% over the control, attributable to the lower water content and the assumed packing bonus; mean-based class B40) with a 28-day capillary porosity of 0.160 versus 0.223 (−28%), lowering the paste-permeability index to about one-third of the control's, and utilizes 120 kg of industrial by-products per cubic meter while avoiding at least 72 kg of binder-related CO_2. The GOST durability grades (frost resistance, water impermeability, abrasion, sulfate resistance) are deliberately not predicted and await the ongoing laboratory campaign; the work is therefore a computational mix-design study with a single measured verification composition.

Keywords: ternary cementitious system, fly ash, silica fume, irrigation canal concrete, particle packing, Bolomey model, Powers model, capillary porosity, industrial by-product utilization.

1. Introduction

Kazakhstan operates more than 13,000 hydraulic structures, including reservoirs, dams and canals, that underpin irrigated agriculture in the country's arid and semi-arid southern regions [1]. A national modernization program has been launched to construct 20 new reservoirs, reconstruct 15 existing ones, and rehabilitate more than 14,000 km of irrigation canals, with the explicit goal of cutting unproductive water-transportation losses from 50% to 25% [1]. More recent assessments from the United Nations Development Programme (February 2026) describe the problem as more severe than the original 50% baseline: overall system losses reach up to 60%, so that of every 1,000,000 m^3 of water abstracted from rivers only 400,000-450,000 m^3 reach farmland against a 700,000 m^3 benchmark, and roughly half of the country's irrigation canals require reconstruction [2]. A World Bank report on the Second Irrigation and Drainage Improvement Project (June 2026) documents progress at project scale: 812.6 km of lined canals, 2,325 km of earthen secondary canals and more than 28,800 hydraulic structures rehabilitated across four southern regions [3], illustrating both the scale of ongoing investment and the volume of canal-lining concrete the sector continues to require.

The service environment of canal trough concrete in this setting is demanding: large seasonal temperature swings of the continental climate drive frequent freeze-thaw cycling of water-saturated concrete, regional groundwaters and soils carry sulfate concentrations reported in the 400-1200 mg/L range [4], and sediment-laden flow abrades the lining surface. Where linings degrade under this combination of stressors, filtration losses through cracked or spalled concrete have been reported to exceed 20-25% of conveyed volume in affected reaches [4], a direct, quantifiable link between concrete durability and the national water-loss figures above.

Partial replacement of Portland cement with supplementary cementitious materials (SCMs) is a standard route to both improved durability and reduced embodied carbon: SCMs reduce the calcium hydroxide content of the hydrated matrix through secondary (pozzolanic) hydration, refine pore structure, and lower permeability, while displacing clinker, the most carbon-intensive constituent of concrete. Global cement industry data (GCCA Getting the Numbers Right database, 2023 dataset) indicate an average of roughly 0.60-0.65 kg of CO_2 per kg of cementitious product [5], a figure consistent with independent IEA estimates of 0.5-0.6 t CO_2 per ton of cement [6]; a 25% reduction in CO_2 intensity per ton of cementitious material has been achieved industry-wide since 1990 [7], but absolute emissions continue to rise with production volume, keeping clinker substitution a priority lever.

Ternary systems that combine Portland cement with two complementary SCMs (typically a coarser, spherical, slow-reacting fly ash of 1-100 μm and an ultrafine, fast-reacting silica fume of 0.1-1 μm) exploit particle-packing and reactivity effects that exceed the sum of the individual materials' contributions; such synergies in strength and durability are well documented internationally for silica-fume-fly-ash ternary cements [8]. At the physical level, the fine silica fume fills the interstitial voids left between coarser cement and fly-ash grains, raising packing density; at the chemical level, silica fume drives rapid early pozzolanic densification while fly ash contributes a slower, longer-lived consumption of portlandite that continues to refine the pore structure well beyond 28 days. Recent Kazakhstani rheological work on the same DSF-95 silica fume source used in this study confirms the same qualitative pattern for local materials: silica fume raises plastic viscosity and accelerates structural build-up through its very high specific surface area, while fly ash lowers both yield stress and viscosity via a spherical, ball-bearing particle effect [9], information directly relevant to placing a ternary mixture in canal trough formwork; air-entraining agents further modify the rheology and freeze-thaw response of such mixtures [10].

Imanov et al. [4] combined Portland, pozzolanic and slag cements with 10% fly ash and 7% silica fume (W/C = 0.35) and, relative to their control concrete, reported increases in compressive strength to 55 MPa (+14.6%), splitting tensile strength to 4.6 MPa (+27.8%), frost resistance from 220 to 320 cycles (+45%), water-impermeability grade from W6 to W9 (+50%), abrasion resistance (+26.9%) and sulfate-resistance coefficient (+11.5%), translating into an estimated 30-40% extension of service life. That composition, however, was developed through engineering iteration rather than a priori packing or strength modeling, and it reduces the clinker demand only modestly (blended-cement substitution, not a direct cement cut). Lekhya and Kumar [11] studied high-performance concretes with ultrafine fly ash and silica fume at up to 15% each in binary and ternary combinations: cement reduction reached 30%, and sorptivity and permeable voids decreased by 15-20%, but frost resistance was not tested, and the cement content of the high-strength base mixtures remained high.

Most existing research has therefore focused either on strength optimization or on individual durability indicators, and few studies have formulated and tested modified concretes specifically for Kazakhstani irrigation-canal service (e.g., [4]); a broader disconnect remains between the multi-component binder-optimization tools now standard in cementitious materials research and their systematic application to irrigation- and hydraulic-durability criteria, in particular to a substantial, direct reduction of clinker demand rather than blended-cement substitution.

It can be hypothesized that replacing 30% of the cement in a working plant mixture with 20% Ekibastuz fly ash and 10% DSF-95 silica fume (binder proportions selected by particle-packing simulation; total binder content, paste volume and aggregate skeleton of the control preserved) will match or exceed the control strength class at 28 days and improve the porosity-based durability

indicators relevant to canal troughs (capillary porosity, estimated permeability), without requiring changes at an existing precast plant beyond powder storage, dosing and air-content control.

The goal of this study is therefore to develop and computationally verify a cement-reduced ternary composition for irrigation canal trough concrete and to quantify its strength development, porosity-based durability indicators, microstructure and resource efficiency. The specific objectives are to (i) quantify the packing and strength consequences of a 30% direct cement reduction compensated by fly ash and silica fume; (ii) derive the porosity-based durability indicators that follow from the calibrated models and specify the GOST durability test program (frost resistance, water impermeability, abrasion, sulfate resistance) against which the design is to be confirmed, with the mixture benchmarked against Imanov et al. [4]; (iii) document the resulting matrix microstructure by scanning electron microscopy; and (iv) quantify the associated reduction in cement demand and binder-related CO_2 emissions.

2. Methods

2.1. Materials

Ordinary Portland cement CEM I 42.5N (Alma cement plant, Almaty, Kazakhstan) served as the primary binder (28-day standard mortar strength 49.1 MPa; specific surface area 326 m^2/kg; median particle size d50 = 17.2 μm; C3S ≈ 60.2%, C3A ≈ 8.1%). The sulfate resistance of the designed mixtures is attributed to the SCM blend and low water-binder ratio rather than to this moderate C3A content, which by itself does not qualify the cement as sulfate-resisting.

Fly ash was obtained by dry collection from the Ekibastuz thermal power plant and is classified as an acidic (low-calcium) ash per GOST 25818-2017 [12], equivalent to ASTM C618 Class F [13]. Its chemical composition (atomic emission analysis): SiO_2 58.5%, Al_2O_3 29.9%, Fe_2O_3 3.5%, CaO 1.78%, MgO 0.73%, K_2O 0.55%, Na_2O 0.17%, SO_3 0.045%, loss on ignition 0.96%; the sum $SiO_2+Al_2O_3+Fe_2O_3$ = 91.9% is characteristic of an acidic low-calcium ash. Physical characteristics: d50 = 27 μm (coarser than the cement by median size, with a broad 1-100 μm range), specific surface area 340 m^2/kg, loose bulk density 700-800 kg/m^3, radon activity 95.1 Bq/kg (below the 370 Bq/kg limit for building materials). Pozzolanic activity by the modified R^3 bound-water test (ASTM C1897 [14]) corresponds to bound water H_{bound} = 12.8% (moderately active pozzolan).

Condensed silica fume DSF-95 (Temirtau, Karaganda region, Kazakhstan; GOST R 58894-2020 [15]), the same source used in the companion rheological study [9], was used as the ultrafine component: amorphous SiO_2 = 96.85%, d50 = 0.15 μm, specific surface area ≈ 18,200 m^2/kg, bulk density 440 kg/m^3.

Quartz sand from the Kapchagai deposit (fineness modulus 2.4) served as fine aggregate, and granite crushed stone from the Malybai quarry (fractions 5-10 and 10-20 mm) as coarse aggregate. A polycarboxylate-ether superplasticizer (Polyplast) was dosed at 1.2-1.5% of binder mass (4.8 kg per 400 kg of binder in the control, 5.0 kg in the ternary mixture); an air-entraining admixture (0.05% of binder) was included in the ternary mixture to secure frost resistance under water-saturated freeze-thaw exposure.

2.2. Mix proportions and design rationale

Two concrete mixtures are compared directly: a plant control mixture representative of current precast practice (cement 400 kg/m^3), and a cement-reduced ternary mixture (hereafter ECON) in which 30% of the cement mass is replaced by fly ash and silica fume at a fixed binder proportion of 70:20:10, while the total binder mass is held equal to the control's cement content (400 kg/m^3). A higher-binder variant of the same 70:20:10 proportion was also examined at the dissertation stage with a separate non-linear model; it is not considered further here because it does not reduce absolute clinker demand and its source model remains unpublished.

Because the true densities of fly ash (2.10 g/cm^3) and silica fume (2.20 g/cm^3) are lower than that of cement (3.10 g/cm^3), 400 kg of ternary binder occupies approximately 18 L more volume than

400 kg of cement; this is compensated by reducing the mixing water from 170 to 152 L (W/B = 0.38 vs W/C = 0.425 for the control), so that the paste volume of both mixtures is identical (299 L/m^3) and the control's aggregate skeleton (crushed stone 1000 kg/m^3, sand 830 kg/m^3) is carried over unchanged. Water dosages are stated in liters, with 1 L taken as 1 kg. The air-entraining admixture targets 4-6% entrained air in the ternary mixture; this volume is not included in the paste balance of Table 1, and Eq. (1) does not correct for it, so the predicted strengths are upper bounds until the air content is measured (Section 3.7). Consequently, the ternary batch volume exceeds 1 m³ by the entrained-air volume (about 4-6%) unless the aggregate content is reduced correspondingly; batch masses will be corrected for the measured air content. This equal-paste-volume design makes the ternary mixture a direct, one-to-one binder substitution transferable to an existing precast plant without aggregate re-qualification, requiring only additional storage and dosing of the two powders and air-content control. The mix proportions are given in Table 1.

Table 1 – Mix proportions of the control and cement-reduced ternary (ECON) concretes

Component	Control, kg/m^3	Ternary (ECON), kg/m^3
Cement CEM I 42.5N	400	280
Fly ash (Ekibastuz)	-	80
Silica fume DSF-95	-	40
Binder total	400	400
Crushed stone (5-10 and 10-20 mm)	1000	1000
Quartz sand	830	830
Water	170	152
Superplasticizer (Polyplast)	4.8	5.0
Air-entraining admixture	-	0.2
W/B (W/C for control)	0.425	0.380
Calculated density (component sum, excl. air), kg/m^3	2405	2387
Paste volume, L/m^3	299	299

2.3. Computational modeling

Particle packing of the ternary binder was simulated using the sequential-deposition “drop-and-roll” algorithm of Visscher and Bolsterli [16], which drops particles one at a time into a bounded domain and lets each roll, without friction or inertia, into the lowest stable position supported by previously deposited particles; the algorithm's reported packing fraction for mono-sized spheres (≈ 0.582) coincides with the value obtained here for the neat-cement control. The cement, fly ash, and silica fume were represented by log-normal particle-size distributions centered at their measured d50 values (17.2, 27, and 0.15 μm, respectively) and truncated at 0.01-60 μm, and the blended distributions of the candidate binder proportions were benchmarked against the modified Andreasen-Andersen (Dinger-Funk) target curve [17], [18]. The target curve $P(D) = (D^q - D_min^q)/(D_max^q - D_min^q)$, was used with a distribution modulus q = 0.25, within the q ≈ 0.19-0.25 range reported for packing-optimized concretes. The packing densities used in Eq. (3) (0.582 for the control, 0.694 for the ternary blend) are those of the dissertation-stage simulation; the control value coinciding with the mono-sized-sphere limit indicates that those settings did not resolve the full polydispersity of the powders, so both values are treated as provisional inputs, and their effect on the predicted strength is isolated in Section 3.1.

Compressive strength was predicted with a modified Bolomey model [19], the original linear cement/water-ratio formulation extended with cementing-efficiency (k-value) factors for the supplementary materials and a packing-density multiplier:

$$R = A \cdot \left(\frac{C_{eff}}{W} - 0.5\right) \cdot f(\rho_{pack}), \quad (1)$$

$$C_{eff} = C + k_{FA} \cdot FA + k_{SF} \cdot SF, \quad (2)$$

$$f(\rho_{pack}) = 1 + 0.55 \cdot \left(\frac{\rho_{pack} - \rho_0}{\rho_0}\right), \quad (3)$$

where: R in Eq. (1) is the compressive strength at 28 days; A is a coefficient calibrated on the measured control strength (44.5 MPa at W/C = 0.425), giving A = 24.0 MPa (with the cement mortar activity R_c = 49.1 MPa, a = A/R_c = 0.49, transferable to other cement batches); C, FA and SF in Eq. (2) are the masses of cement, fly ash and silica fume, kg/m^3; W is the mixing water content, L/m^3; k_{SF} = 2.0 and k_{FA} = 0.40 at 28 days (consistent with the k-value concept of EN 206 [20] and with values compiled for low-calcium fly ash and condensed silica fume [21]), rising to 0.75 at 90 days to represent the delayed pozzolanic contribution of low-calcium fly ash; and in Eq. (3), f(ρ_{pack}) is the packing-density multiplier, with ρ_{pack} = 0.582 for the control and 0.694 for the ternary blend, ρ_0 = 0.582, and an assumed damping coefficient of 0.55 that is not independently calibrated (Section 3.7). Because the standard-cured laboratory control companion gave the same 28-day mean as the heat-cured plant control (44.5 MPa; Section 2.4), the calibration applies to standard-cured conditions. The model was then checked against the separately tested laboratory composition with the same binder masses as the ternary mixture (cement 280 / fly ash 80 / silica fume 40 kg/m^3, water 158 L): it predicts 52.6 MPa against 52.8 MPa measured. This is a single-point consistency check rather than an independent validation: the calibration lies at W/C = 0.425, the check at W/B = 0.395, and the ECON prediction at W/B = 0.380 is a marginal extrapolation beyond both. In the national Bolomey-Skramtaev formulation the linear branch applies for C/W ≤ 2.5, which the effective C/W of the ECON mixture at 28 days (≈2.58) marginally exceeds; the linear form is retained for consistency with both reference points (2.35 and 2.48); applying the high-C/W branch with continuity at C/W = 2.5 would lower the prediction to about 54.5 MPa, so the reported 55.2 MPa may overestimate the linear-branch result by about 1%.

Strength development with age was described using the fib Model Code 2010 kinetics function [22]:

$$R(t) = R_{28} \cdot \exp[s \cdot (1 - \sqrt{\frac{28}{t}})], \quad (4)$$

where: s in Eq. (4) was fitted to the anchor points: s = 0.15 for the control (a two-point fit to its measured plant values) and s = 0.51 for the ternary mixture, the latter reflecting slowed early clinker kinetics at 30% dilution and lying outside the s = 0.20-0.38 range tabulated in fib MC2010 for neat cements; the ECON 7-day anchor (33.1 MPa) is itself a model estimate of 0.60·R_{28} rather than a measurement. For ages beyond 28 days, the trajectory was interpolated in log time between the 28-day value and a 90-day target from the same Bolomey model with k_{FA} = 0.75, rather than extrapolated from the 7/28-day fit; the control's 90-day value, in contrast, follows the fib fit through its two measured points, an asymmetry acknowledged in Section 3.7. This avoids the early-age dilution slope of the fitted curve overstating the late-age pozzolanic gain.

Durability-related indicators were estimated from Powers' model [23], [24]: the gel-space ratio, Eq. (5),

$$X = \frac{0.68\alpha}{0.32\alpha + W/B}, \quad (5)$$

with compressive strength taken as approximately proportional to X^3, and the capillary porosity, Eq. (6),

$$p = \frac{W/B - 0.36\alpha}{W/B + 0.32}, \quad (6)$$

where: α in Eqs. (5) and (6) is the effective degree of hydration, taken as a base value by age (0.55 at 7 d, 0.72 at 28 d, 0.82 at 90 d) plus 0.08 per unit SCM fraction and capped at α_{max} = 0.95·(W/B)/0.36 so that the gel-space ratio cannot exceed 1; these are assumed values, not measurements, and Powers' relations were derived for neat Portland paste, so the porosity values are indicative for SCM systems. The relative permeability index was taken proportional to $p^3/(1-p)^2$ per Kozeny-Carman; since p ≤ 0.23 for both mixtures, the p^3 presentation retained in Section 3.3 is a close approximation (the full expression changes the ECON/control ratio from 37% to 32%). The binder proportions themselves were selected by computational screening of ten candidate ternary compositions within the ranges of fly ash 0-20% and silica fume 0-10% by binder mass, with the predicted R_{28} of each candidate being obtained by the modeling procedure described above. The 70:20:10 proportion gave the highest

predicted strength; it lies on the boundary of the screened region, so higher fly ash contents were not explored, and it was checked experimentally at a single point (Section 2.4; 52.8 MPa measured).

2.4. Specimen preparation and mechanical testing

Concrete was mixed in a laboratory forced-action mixer in the following sequence: aggregates, cement and mineral additions, 70% of the water, then the superplasticizer with the remaining 30% of the water. Cubic specimens of size 100×100×100 mm were cast in two layers with vibration compaction and cured in a normal-curing chamber (20 ± 2 °C, RH ≥ 95%). The laboratory campaign covered the validation composition (cement 280 / fly ash 80 / silica fume 40 kg/m^3, water 158 L; Section 2.3), which did not include the air-entraining admixture, together with a laboratory control companion with the plant control proportions of Table 1 (cement 400 kg/m^3, water 170 L, superplasticizer 4.8 kg/m^3, no SCMs). Both were cast on 2 May 2026 and cured identically: nine cubes of the validation composition, tested in threes at 7, 14 and 28 days, and three control cubes, tested at 28 days (44.5 MPa, mean of three). All cubes were tested on a calibrated CONTROLS PILOT hydraulic compression press (CONTROLS S.r.l., Milan, Italy; calibration certificate no. BA-03-25-3130343, valid until 4 June 2026) at a loading rate of 0.6 MPa/s per GOST 10180-2012 [25]; the 28-day compression tests of 30 May 2026 fall within the calibration validity, and fracture fragments for SEM were sampled on 5 June 2026 and examined on 12 June 2026 (Section 2.6). The control-mixture results at 2 and 28 days are plant quality-control data obtained on 100×100×100 mm cubes from three production series, heat-cured under the plant regime (28-day mean 44.5 MPa, equal to that of the laboratory control companion); the early-age control values therefore reflect steam curing, whereas all laboratory values are standard-cured, which limits the comparability of early-age strengths (Sections 3.1 and 3.7). The ECON mixture of Table 1 was not cast at this stage: its values in Table 2 and Figure 1 are model outputs obtained by the procedure of Section 2.3, and the durability tests of Section 2.5 form the ongoing campaign. Splitting tensile strength was estimated from the mean cube strength as $f_{sp} = 0.30 \cdot R_{28}^{(2/3)} \cdot (1 + 0.08 \cdot f_{SCM})$, where f_{SCM} is the SCM mass fraction of the binder (0 for the control, 0.30 for ECON), i.e., the EN 1992-1-1 relation $f_{ctm} = 0.30 \cdot f_{ck}{}^{(2/3)}$ [26] applied to R_{28} without cube-to-cylinder conversion, with a densification allowance of 8% per unit SCM fraction (2.4% for ECON), pending direct splitting tests.

2.5. Durability testing program

The durability program targets the service profile described in the Introduction: frost resistance by GOST 10060-2012, second accelerated method [27]; water impermeability by GOST 12730.5-2018 [28]; abrasion resistance by GOST 13087-2018 [29]; and sulfate resistance within the exposure classification of GOST 31384-2017 [30], the coefficient being determined from specimen strength after sulfate-solution storage relative to water storage. GOST frost grade F denotes the number of sustained freeze-thaw cycles, and impermeability grade W the water pressure withstood in 0.1 MPa steps. The GOST 13087 abrasion value will be reported as a general wear indicator rather than a prediction of erosion by sediment-laden flow, which would require an underwater abrasion method (e.g., ASTM C1138/C1138M [31]). Given the low winter temperatures, the campaign design includes combined freeze-thaw and sulfate exposure, the air-void system (spacing factor per ASTM C457/C457M [32]), and the thaumasite form of sulfate attack. These grades are treated strictly as test targets and not as model outputs: no validated quantitative relation from mix proportions or computed porosity to the GOST frost, impermeability, abrasion or sulfate-resistance grades is available for these materials, so the laboratory campaigns, in progress at the time of drafting, are the only admissible source of these values.

2.6. Microstructural analysis

Fracture surfaces of 41-day specimens of the laboratory-cast control companion (same cement, no SCMs) and of the validation composition (binder proportions identical to the ECON mixture, with Karaganda DSF-95 silica fume, water 158 L; Section 2.4) were examined by scanning

electron microscopy on a JEOL JCM-7000 (NeoScope) benchtop instrument (JEOL Ltd., Tokyo, Japan) in secondary-electron detection mode at an accelerating voltage of 10 kV, working distances of 11.4-15.2 mm and high vacuum, without conductive coating, at magnifications from ×500 to ×4,000; representative micrographs at ×500 and ×1,000 are discussed in Section 3.4. Fragments were sampled from the cubes tested in compression on 30 May 2026 and imaged on 12 June 2026; matrix compactness, visible porosity, and the morphology of hydration products and residual SCM particles were compared between the two mixtures at matched magnifications.

3. Results and Discussion

3.1. Compressive strength development and model check

The predicted strength development of the two mixtures is presented in Figure 1 and summarized in Table 2.

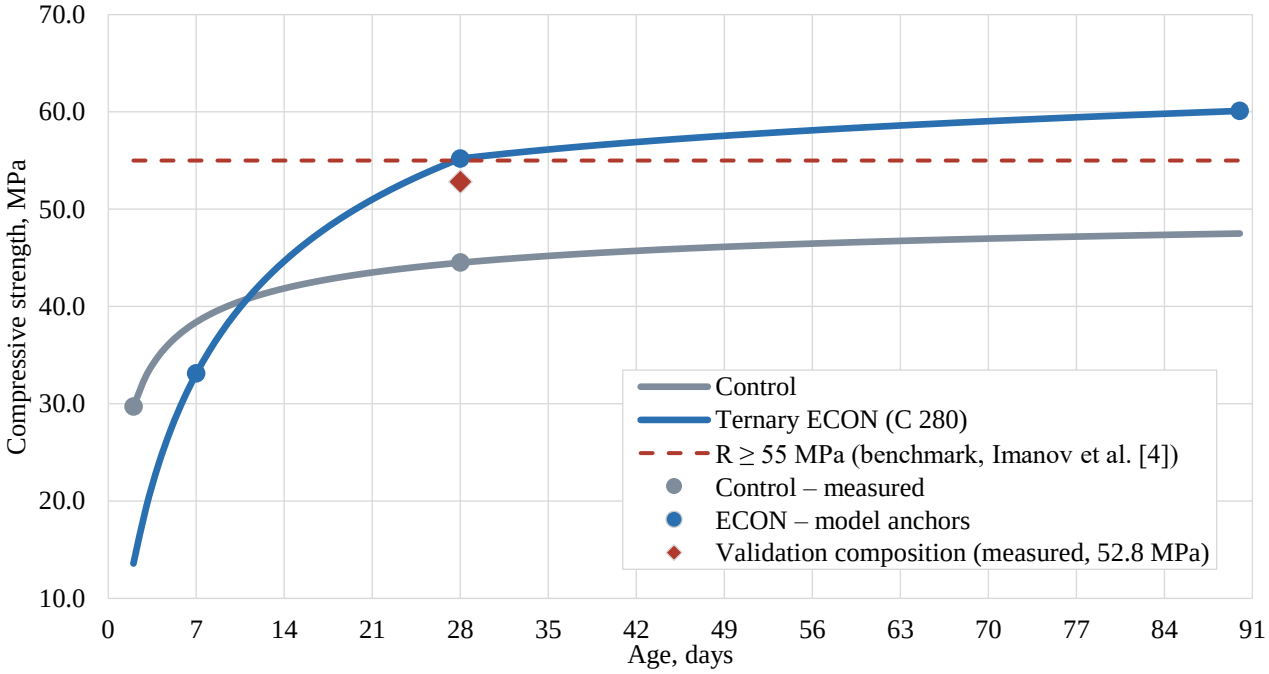


Figure 1 – Predicted compressive-strength development of the control and cement-reduced ternary (ECON, cement 280 kg/m^3) mixtures. Markers denote measured values (control at 2 and 28 days; validation composition at 28 days, filled diamond) or model anchor points (Sections 2.3 and 2.4). The dashed line is the 55 MPa benchmark strength of Imanov et al. [4]

Table 2 – Compressive strength by age (control: 2- and 28-day values are measured, the 28-day mean being identical for the heat-cured plant series and the standard-cured laboratory companion; 7-, 14- and 90-day control values follow the fib fit, Eq. (4); ECON: model outputs, Section 2.3)

Age, days	Control, MPa	Ternary ECON, MPa
2	29.7 (measured)	13.6
7	38.4	33.1
14	41.9	44.7
28	44.5 (measured)	55.2
90	47.5	60.1

As shown in Figure 1, at 28 days the ECON mixture is predicted to reach 55.2 MPa, a mean-based class B40 (+24% over the control's B30; per GOST 18105-2018 [33], class assignment requires the coefficient of variation, and at the standard CV = 13.5% B40 requires a mean of at least 51.4 MPa, which 55.2 MPa satisfies; B40 corresponds approximately to C32/40 per EN 206), despite a 30%

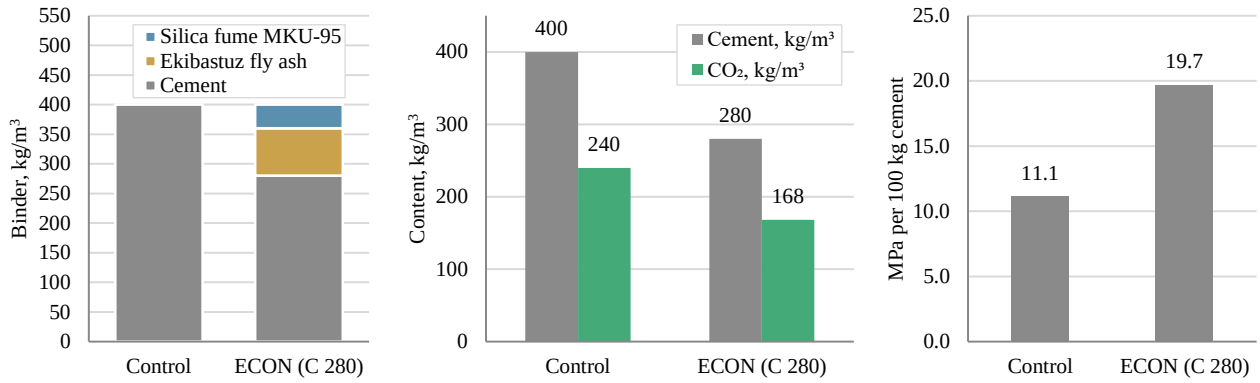
reduction in cement content, and the margin widens further by 90 days (60.1 vs 47.5 MPa, +27%). The predicted early-age strength (13.6 MPa at 2 days, standard-cured) is markedly lower than the control's plant-measured 29.7 MPa, reflecting the dilution of reactive clinker at 30% total SCM replacement before the pozzolanic contribution matures; this value follows from the assumed 7-day ratio of $0.60 \cdot R_{28}$ rather than from an independent prediction. The resulting crossover at roughly 10-14 days in Figure 1, after which the ternary curve overtakes the control, is consistent in kind with the age-dependent dilution-reaction-synergy sequence reported for fly-ash-silica-fume systems [9], [11]. The model reproduces the separately tested composition sharing the ECON binder proportions to within 0.4% (52.6 MPa predicted vs 52.8 MPa measured; Section 2.3). The predicted gain can be decomposed as follows. At the same water content (152 L), a neat-cement mixture with 400 kg/m^3 of cement would reach ≈51.2 MPa by Eq. (1), i.e., +6.7 MPa over the control from water reduction alone. Replacing 120 kg of cement with fly ash and silica fume at their k-values gives an effective cement content of 392 kg/m^3 and ≈49.9 MPa, about 1.3 MPa below the neat mixture at equal water. The packing multiplier then adds ≈5.3 MPa. The predicted gain therefore stems from the reduced water content and the assumed packing bonus, not from 28-day SCM chemistry. Splitting tensile strength, estimated by the correlation in Section 2.4, is 4.45 MPa for the ECON mixture versus 3.77 MPa for the control (an 18% difference that follows directly from the correlation and is not an experimental finding), still marginally below the 4.6 MPa measured for the benchmark mixture of [4]. The laboratory testing of the validation composition is documented in Figure 2.



Figure 2 – Compression testing of the validation composition on the calibrated CONTROLS PILOT press: cube No. 5 in the test position between the platens (the specimen number is marked on the formed face before loading, per GOST 10180-2012 [25]); its 28-day result (52.8 MPa) serves as the single-point consistency check of Section 2.3.

3.2. Resource efficiency and embodied carbon

Figure 3 compares the binder structure, cement demand with the associated CO_2 footprint, and cement efficiency of the two mixtures.



a) Binder structure

b) Cement content and CO_2 footprint

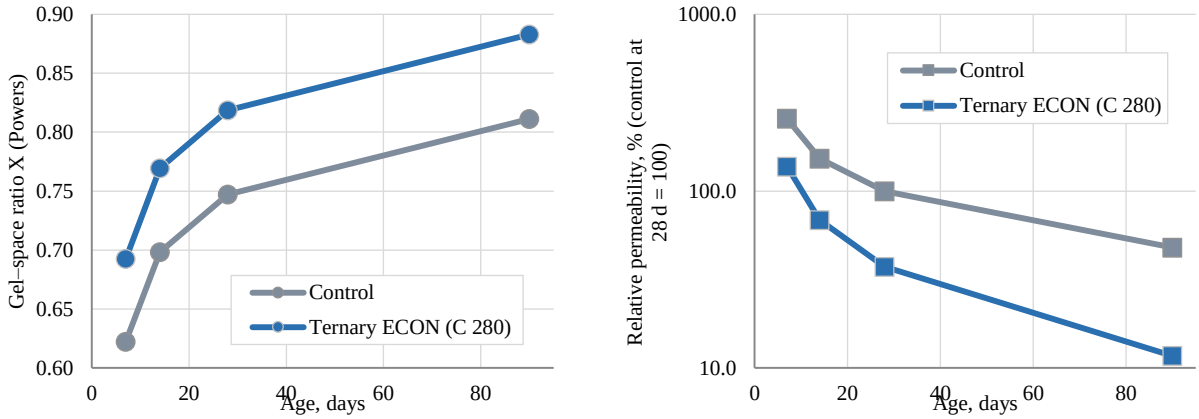
c) Cement efficiency (R_{28} per cement content)

Figure 3 – Comparison of binder structure, cement demand, associated CO_2 footprint, and cement efficiency of the two mixtures (28-day strength delivered per 100 kg of cement)

The ECON design uses 120 kg less cement per cubic meter than the control (−30%) while utilizing 120 kg/m^3 of industrial by-products (80 kg fly ash + 40 kg silica fume). Using the GNR industry-average factor of 0.60 kg CO_2 per kg of cementitious product [5] (a lower bound for a CEM I cement, whose clinker content is higher), this corresponds to a reduction of at least ≈72 kg of binder-related CO_2 per cubic meter (cradle-to-gate, excluding transport and by-product allocation). Cement efficiency, taken as 28-day strength per 100 kg of cement, rises from 11.1 MPa (control) to 19.7 MPa (ECON), a 77% improvement.

3.3. Powers-model porosity and relative permeability

Because no validated relation from mix design or computed porosity to the GOST durability grades exists for these materials (Section 2.5), the durability-related results are confined to the quantities that do follow from the calibrated models: the gel-space ratio and the relative water permeability by age, presented in Figure 4.



a) Gel-space ratio (Powers model); strength ∝ X^3

b) Relative water permeability (∝ capillary porosity^3)

Figure 4 – Powers-model indicators of the control and ternary (ECON) mixtures from 7 to 90 days (the permeability index in (b) is normalized to the control at 28 days (= 100%) and plotted on a log scale; p^3 approximates the full Kozeny-Carman form $p^3/(1-p)^2$ closely at these porosities)

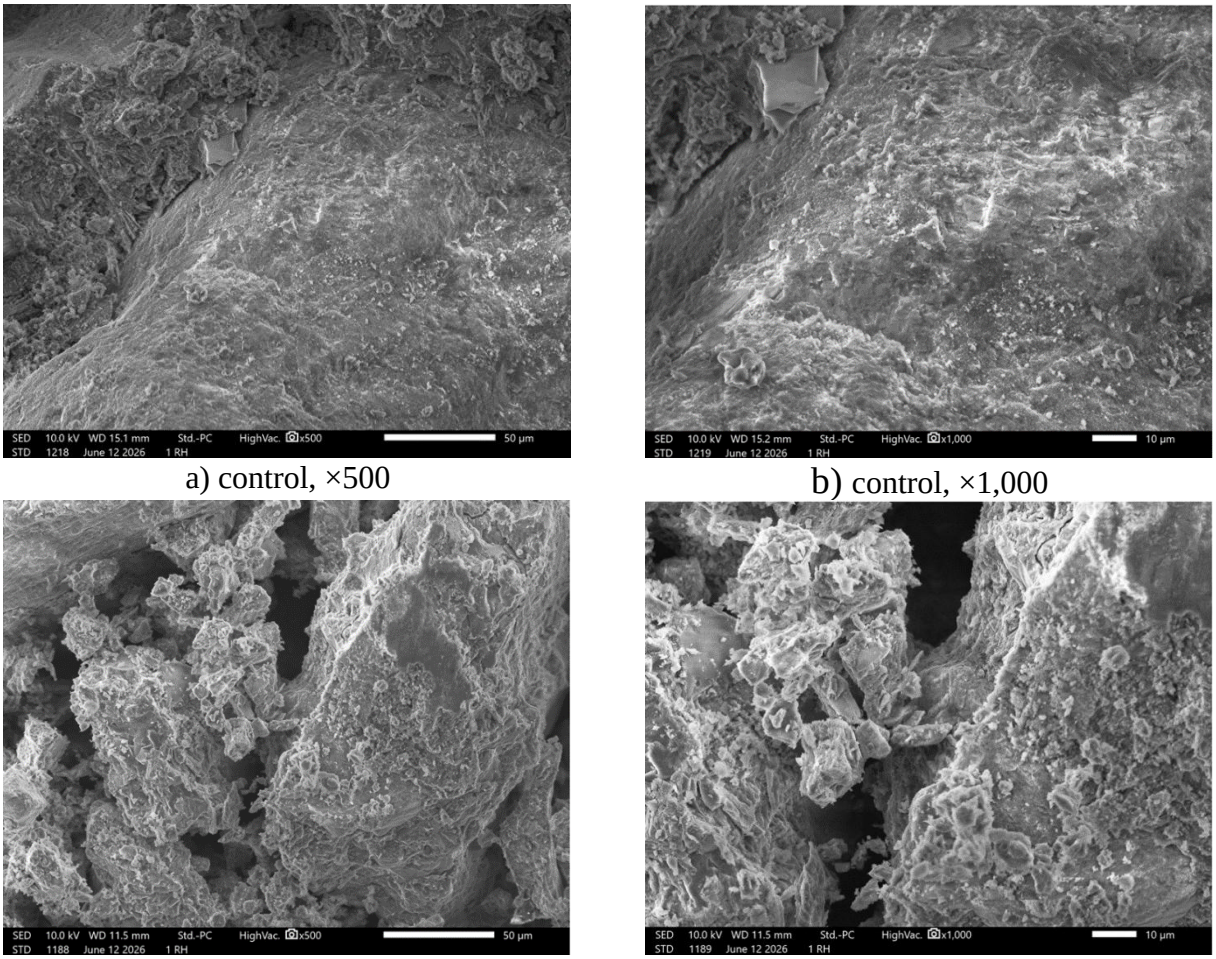
As shown in Figure 4a, the gel-space ratio of the ECON mixture exceeds that of the control at every age (7 to 90 days), reflecting its lower W/B despite the cement dilution, by a nearly constant margin ($\Delta X \approx 0.07$ at 7, 28 and 90 days), because the model applies an age-independent SCM increment to α, so age-dependent pozzolanic gains aren't captured. Capillary porosity at 28 days falls

from 0.223 (control) to 0.160 (ECON), consistent with a 37% relative permeability index (100% = control at 28 days; 32% with the full Kozeny-Carman form): the ECON mixture's index at 28 days is thus roughly a third of the control's, easing to about a quarter by 90 days as both mixtures continue to densify. These are paste-level indicators and neglect the interfacial transition zone and entrained air.

3.4. Microstructure

Fracture surfaces of the control companion and of the validation composition (binder identical to ECON) at matched magnifications are shown in Figure 5.

At ×500 the control (Figure 5a) shows a compact, continuous fracture surface with few open voids; at ×1,000 (Figure 5b) the same field shows a smooth but locally loose fabric with angular relics and scattered fine debris. The validation composition at ×500 (Figure 5c) shows a more heterogeneous surface, with clustered hydration products and residual particles separated by open voids several tens of micrometers across; at ×1,000 (Figure 5d) the clusters show a fine granular texture and an isolated microcrack along the fracture path. On these single fields, no clear difference in matrix density between the two mixtures can be established, and fracture-surface topography is not a reliable indicator of porosity. The comparison is qualitative, based on one representative field per mixture, and phase identification at these magnifications is tentative without EDS; quantitative follow-up (BSE imaging of polished sections, EDS mapping, porosimetry) is identified in Section 3.7.



a) control, ×500 b) control, ×1,000

c) validation composition (ECON binder), ×500 d) validation composition (ECON binder), ×1,000

Figure 5 – SEM micrographs (JEOL JCM-7000, SED mode, 10 kV) of 41-day fracture surfaces, ordered by magnification

3.5. Comparison with previous studies

Table 3 places the ECON mixture alongside the benchmark Kazakhstani irrigation-canal study [4] and the ultrafine-fly-ash-silica-fume high-performance-concrete study [11], which used a similar total SCM replacement level.

Table 3 – Comparison with the two most directly relevant prior studies; the GOST durability grades of the ECON mixture are the subject of the ongoing campaign (Section 2.5)

Study	SCM system	Cement reduction	R_{28}, MPa	Frost	Impermeability
This study (ECON)	70% C + 20% FA + 10% SF	−30% (400→280 kg/m^3)	55.2 (model)	in progress	in progress
Imanov et al. [4]	Multi-cement + 10% FA + 7% SF	≈−17% (blend)	55 (measured)	320 cycles (measured)	W9 (measured)
Lekhya and Kumar [11]	UFFA + SF, ≤15% each (binary/ternary)	−30%	wide range (HPC)	not tested	reduced sorptivity, −15-20% permeable voids

The ECON mixture is predicted to essentially match the measured 28-day strength of the benchmark concrete (55.2 vs 55 MPa) while remaining marginally below its splitting tensile strength (4.45 vs 4.6 MPa); a direct comparison of frost-resistance and impermeability grades is not yet possible, because the corresponding GOST campaign for the ternary system is still in progress (Section 2.5). The ECON design achieves its position with a direct 30% cement cut (roughly 1.8 times the ≈17% blended substitution of [4]) via a design workflow (particle-packing simulation coupled to a strength model checked against a measured composition) that neither [4] nor the broader Kazakhstani SCM literature [9], [10] has yet applied to the irrigation-durability problem. Lekhya and Kumar [11] achieved a comparable 30% cement reduction with a similar total SCM content and reported a 15-20% finer pore structure, but did not test frost resistance, so the porosity-based estimates of the present study cannot be benchmarked against their data.

3.6. Implications for irrigation canal practice

Because the paste volume and aggregate skeleton of the control mixture are preserved (Section 2.2), the ECON mixture can be introduced at existing precast plants as a direct binder substitution without aggregate re-qualification, with only powder storage, dosing, and air-content control added. Its reduced capillary porosity and estimated water permeability (Section 3.3), combined with a predicted class B40 strength, provide favorable durability indicators for canal-trough service, although the definitive GOST grades must still be established by the ongoing campaigns (Section 2.5). The cement saving is directly relevant to the scale of rehabilitation described in the Introduction (more than 14,000 km of canals nationally; 812.6 km of lined canals in the World Bank-supported project alone [3]): a 30% per-cubic-meter cement saving compounds into a substantial reduction in clinker demand and binder-related CO_2 across the program, while using Ekibastuz fly ash and Karaganda silica fume that would otherwise remain industrial by-products. At a representative lining volume of 500 m^3 per kilometer of canal (range 200-1,200 m^3/km, from precast flumes to lined main canals), the 120 kg/m^3 cement saving corresponds to ≈60 t of cement and ≈36 t of CO_2 avoided per kilometer. Applied to the full 14,000 km national program, this gives an upper bound of the order of 0.5 Mt CO_2 (range 0.2-1.2 Mt); since only part of the rehabilitated network will receive concrete lining (about one quarter in the World Bank-supported project [3]), a realistic estimate is of the order of 0.1-0.2 Mt CO_2 (assumptions: 0.60 kg CO_2 per kg of cementitious product; lining geometry as stated).

3.7. Limitations and further work

Several limitations qualify these findings. First, no GOST durability grades (frost resistance, water impermeability, abrasion, sulfate resistance) are predicted or reported for the designed mixtures: no validated quantitative relation from mix proportions or computed porosity to these

grades exists for the local materials, so the ongoing campaigns of Section 2.5 are the only admissible source of these values, and the durability conclusions of this study are accordingly confined to the porosity-based indicators of Section 3.3. Moreover, the laboratory program reported here covers a single measured composition, the validation mix sharing the ECON binder proportions (Section 2.4), three companion cubes per age; individual cube readings, their dispersion, and the 7- and 14-day means are not reported, so the strength values should be interpreted as indicative means until a dedicated statistical series, including the ECON mixture itself, is completed. The strength model also rests on provisional packing densities and an uncalibrated packing-damping coefficient (0.55, Eq. (3)), and the 90-day values are obtained differently for the two mixtures (fib extrapolation for the control, Bolomey with k_{FA} = 0.75 for ECON); both choices affect the predicted margin and will be revisited with the ECON test data. Second, the predicted early-age penalty (2-day strength roughly half the control's heat-cured plant value) is an inherent consequence of 30% clinker replacement; given that the plant already heat-cures its control concrete, this will need to be verified under the plant's steam-curing regime before industrial implementation. Third, fresh-state properties (slump or flow, air content, setting time) have not yet been measured: at W/B = 0.38 with 10% silica fume, the mixture may require superplasticizer adjustment for trough placement, and the 4-6% target air content will reduce the predicted strength accordingly; these data accompany the casting campaign. Fourth, thin canal linings are cracking-sensitive: silica fume at low W/B raises autogenous-shrinkage and plastic-shrinkage cracking risk under the hot, dry conditions described in the Introduction, so shrinkage measurements, and field curing requirements are included in the follow-up. Fifth, the estimated splitting tensile strength falls marginally short of the 4.6 MPa benchmark of [4]; dispersed polypropylene micro-fiber is a direct candidate remedy. Sixth, the SEM comparison of Section 3.4 is qualitative, based on one field per mixture, without EDS; BSE imaging of polished sections, elemental mapping and porosimetry would allow quantitative comparison with the Powers-model porosity estimates of Section 3.3. Finally, batch-to-batch variability of the Ekibastuz ash and DSF-95 (fineness, loss on ignition, amorphous content) requires plant acceptance criteria and verified regional availability, and long-term field validation on an operating canal section remains the decisive test of the laboratory and modeling results reported here.

4. Conclusions

1. A ternary binder combining Portland cement CEM I 42.5N, Ekibastuz low-calcium fly ash and Karaganda DSF-95 silica fume (70:20:10) was designed by particle-packing simulation and a Bolomey strength model checked to within 0.4% against a measured composition, replacing 30% of the cement of a plant control mixture (280 vs 400 kg/m^3) while holding the total binder content, paste volume and aggregate skeleton unchanged.

2. The cement-reduced ternary composition is predicted to reach mean-based class B40 (R_{28} = 55.2 MPa, a 24% increase over the control, attributable to the lower water content and the assumed packing bonus) with an estimated 18% higher splitting tensile strength (4.45 vs 3.77 MPa, correlation-borne); the predicted early-age strength is roughly halved (13.6 vs a heat-cured plant value of 29.7 MPa at 2 days), which will need verification under the plant’s steam-curing regime or a delayed formwork-removal schedule.

3. The 28-day capillary porosity decreases from 0.223 to 0.160 (−28%), lowering the estimated relative water permeability to about one third of the control's; the GOST durability grades (frost resistance, water impermeability, abrasion, sulfate resistance) were deliberately not predicted (no validated relation from computed mix properties to these grades exists for the local materials) and are the subject of the ongoing test program (Section 2.5).

4. SEM of fracture surfaces did not show a conclusive difference in matrix density between the control and the validation composition at the magnifications examined; BSE imaging of polished sections, EDS, and porosimetry are required to test the porosity reduction predicted by the Powers model.

5. Per cubic meter, the mixture utilizes 120 kg of industrial by-products and cuts binder-related CO_2 by at least 72 kg, and can be adopted at existing precast plants as a direct binder substitution requiring only powder storage, dosing, and air-content control.

6. Determination of the frost-resistance and impermeability grades within the ongoing laboratory campaign, fiber reinforcement to close the splitting-tensile margin, and field validation on an operating canal section are the immediate next steps toward application.

References

[1] "Annual Results: Water Infrastructure Development and Technology Implementation for Sustainable Future of Kazakhstan," Official Information Source of the Prime Minister of the Republic of Kazakhstan. Accessed: Sep. 20, 2026. [Online]. Available: https://primeminister.kz/en/news/reviews/annual-results-water-infrastructure-development-and-technology-implementation-for-sustainable-future-of-kazakhstan-29470

[2] "Kazakhstan advances modernization and digitalization of the water sector with support from international partners," UNDP Kazakhstan. Accessed: Sep. 25, 2026. [Online]. Available: https://www.undp.org/kazakhstan/press-releases/kazakhstan-advances-modernization-and-digitalization-water-sector-support-international-partners

[3] "Kazakhstan's Irrigation Overhaul: Less Waste, Better Harvests," World Bank Group.

[4] A. M. Imanov, Zh. N. Moldamuratov, O. D. Seitkazinov, A. Z. Tukhtamisheva, A. B. Ismailova, and G. M. Rakhimova, "Enhanced operational reliability of irrigation canals through the application of modified concrete," *Nanobuild*, vol. 17, no. 6, pp. 678–696, 2025, doi: 10.15828/2075-8545-2025-17-6-678-696.

[5] "GNR 2.0 – GCCA in Numbers," GCCA. Accessed: Sep. 25, 2026. [Online]. Available: https://gccassociation.org/gnr/

[6] "Cement. Production, energy demand and emissions," IEA. Accessed: Sep. 25, 2026. [Online]. Available: https://www.iea.org/energy-system/industry/cement

[7] "Cement and Concrete Industry Net Zero Action and Progress Report," GCCA. Accessed: Sep. 25, 2026. [Online]. Available: https://gccassociation.org/cement-and-concrete-industry-net-zero-action-and-progress-report/

[8] M. D. A. Thomas, M. H. Shehata, S. G. Shashiprakash, D. S. Hopkins, and K. Cail, "Use of ternary cementitious systems containing silica fume and fly ash in concrete," *Cement and Concrete Research*, vol. 29, no. 8, pp. 1207–1214, Aug. 1999, doi: 10.1016/S0008-8846(99)00096-4.

[9] Z. Zhumadilova *et al.*, "Rheological, Thermal, and Microstructural Behavior of Cementitious Systems with Silica Fume and Fly Ash for Self-Compacting Concrete," *J. Compos. Sci.*, vol. 10, no. 7, p. 341, Jun. 2026, doi: 10.3390/jcs10070341.

[10] A. Tolegenova, G. Skripkiunas, L. Rishko, and K. Akmalaiuly, "Air-Entraining Effect on Rheological Properties of Cement-Based Mixtures," *Advances in Materials Science and Engineering*, vol. 2024, no. 1, p. 5018973, Jan. 2024, doi: 10.1155/2024/5018973.

[11] A. Lekhya and N. S. Kumar, "A study on the effective utilization of ultrafine fly ash and silica fume content in high-performance concrete through an experimental approach," *Heliyon*, vol. 10, no. 22, p. e39678, Nov. 2024, doi: 10.1016/j.heliyon.2024.e39678.

[12] "GOST 25818-2017 Thermal plant fly-ashes for concretes. Specifications," Moscow, Russia: Standardinform, 2017, p. 19.

[13] *ASTM C618-23e1 Specification for Coal Ash and Raw or Calcined Natural Pozzolan for Use in Concrete*, Philadelphia, PA, USA., 2023. doi: 10.1520/C0618-23E01.

[14] *ASTM C1897-20 Standard Test Methods for Measuring the Reactivity of Supplementary Cementitious Materials by Isothermal Calorimetry and Bound Water Measurements*, Philadelphia, PA, USA., 2020. doi: 10.1520/C1897-20.

[15] "GOST R 58894-2020 Silica Fume for Concretes and Mortars. Specifications," Moscow, Russia: Standardinform, 2020, p. 19.

[16] W. M. Visscher and M. Bolsterli, "Random Packing of Equal and Unequal Spheres in Two and Three Dimensions," *Nature*, vol. 239, no. 5374, pp. 504–507, 1972, doi: 10.1038/239504a0.

[17] A. H. M. Andreasen, "Ueber die Beziehung zwischen Kornabstufung und Zwischenraum in Produkten aus losen Körnern (mit einigen Experimenten)," *Kolloid-Zeitschrift*, vol. 50, no. 3, pp. 217–228, 1930, doi: 10.1007/BF01422986.

[18] J. E. Funk and D. R. Dinger, *Predictive Process Control of Crowded Particulate Suspensions*. Boston, MA: Springer US, 1994. doi: 10.1007/978-1-4615-3118-0.

[19] J. Bolomey, "Granulation et prévision de la résistance probable des bétons," *Travaux*, vol. 19, no. 30, pp. 228–232.

[20] "EN 206:2013+A1:2016 Concrete - Specification, performance, production and conformity," Brussels, Belgium: CEN, 2016, p. 102.

[21] V. G. Papadakis and S. Tsimas, "Supplementary cementing materials in concrete," *Cement and Concrete Research*, vol. 32, no. 10, pp. 1525–1532, 2002, doi: 10.1016/S0008-8846(02)00827-X.

[22] Fib, *fib Model Code for Concrete Structures 2010*, 1st ed. Wiley, 2013. doi: 10.1002/9783433604090.

[23] T. C. Powers and T. L. Brownyard, "Studies of the Physical Properties of Hardened Portland Cement Paste," *JP*, vol. 43, no. 9, pp. 249–336, 1946, doi: 10.14359/15302.

[24] T. C. Powers, "Structure and Physical Properties of Hardened Portland Cement Paste," *Journal of the American Ceramic Society*, vol. 41, no. 1, pp. 1–6, 1958, doi: 10.1111/j.1151-2916.1958.tb13494.x.
[25] "GOST 10180-2012 Concretes. Methods for strength determination using reference specimens," Moscow, Russia: Standardinform, 2012, p. 36.
[26] "EN 1992-1-1 Eurocode 2: Design of concrete structures - Part 1-1: General rules and rules for buildings," Brussels, Belgium: CEN, 2004, p. 225.
[27] "GOST 10060-2012 Concretes. Methods for determination of frost-resistance," Moscow, Russia: Standardinform, 2018, p. 24.
[28] "GOST 12730.5-2018 Concretes. Methods for determination of water tightness," Moscow, Russia: Standardinform, 2019, p. 19.
[29] "GOST 13087-2018 Concretes. Methods of abrasion test," Moscow, Russia: Standardinform, 2018, p. 16.
[30] "GOST 31384-2017 Protection of concrete and reinforced concrete structures against corrosion. General technical requirements," Moscow, Russia: Standardinform, 2018, p. 49.
[31] *ASTM C1138M-19 Test Method for Abrasion Resistance of Concrete (Underwater Method)*, Philadelphia, PA, USA., 2019. doi: 10.1520/C1138M-19.
[32] *ASTM C457/C457M-24 Test Method for Microscopical Determination of Parameters of the Air-Void System in Hardened Concrete*, Philadelphia, PA, USA., 2024. doi: 10.1520/C0457_C0457M-24.
[33] "GOST 18105-2018 Concretes. Rules for control and assessment of strength," Moscow, Russia: Standardinform, 2018, p. 15.

Information about authors:
Zhuldyz Baikhojayeva – PhD Student, Department of Construction and Building Materials, Satbayev University, Almaty, Kazakhstan, baikhojayeva.z@stud.satbayev.university
Daniyar Akhmetov – Doctor of Technical Sciences, Professor, Department of Construction and Building Materials, Satbayev University, Almaty, Kazakhstan, d.a.akhmetov@satbayev.university
Khrystyna Moskalova – PhD, Assistant Professor, Development and Training Centre for the Metal Industry – Metal Centre Čakovec, Čakovec, Croatia, kristina@metalskajezgra.hr

Author Contributions:
Zhuldyz Baikhojayeva – conceptualization, methodology, software, data curation, formal analysis, investigation, writing-original draft preparation, and visualization.
Daniyar Akhmetov – supervision, project administration, resources, and writing-review and editing;
Khrystyna Moskalova – international supervision, project administration, resources, and writing-review and editing.

Conflict of Interest: The authors declare no conflict of interest.

Use of Artificial Intelligence (AI): The authors declare that AI-assisted tools were used for language editing.

Received: 06.09.2026
Revised: 07.11.2026
Accepted: 13.11.2026
Published: 15.11.2026

Copyright: © 2026 by the authors. Licensee Technobius, LLP, Astana, Republic of Kazakhstan. This article is an open access article distributed under the terms and conditions of the Creative Commons Attribution (CC BY-NC 4.0) license (https://creativecommons.org/licenses/by-nc/4.0/).